Polarization and Trapping of Weakly Bound Atoms in Penning Trap Fields

S. G. Kuzmin and T. M. O'Neil
Department of Physics, University of California at San Diego, La Jolla, California 92093, USA
(Received 10 October 2003; published 17 June 2004)

The ATHENA and ATRAP groups at CERN recently reported the production of weakly bound antihydrogen atoms in a non-neutral positron-antiproton plasma. This Letter derives an equation of motion for weakly bound atoms in the electric and magnetic fields of the plasma and trap. The atoms are polarized by the electric field and can be trapped radially in the edge region of the plasma where the electric field is maximum.

DOI: 10.1103/PhysRevLett.92.243401 PACS numbers: 36.10.–k

The ATHENA and ATRAP collaborations at CERN have reported the production of antihydrogen atoms [1,2]. The atoms are produced by recombination when antiprotons are added to a cold (few degrees kelvin) positron plasma. The ATRAP collaboration measured atom binding energies in the range of a few meV [3], and one expects that ATHENA also produced atoms with binding energy in this range, although more deeply bound atoms may have been produced as well. Here, we focus on the weakly bound atoms.

Because the atoms are very weakly bound (few meV) and reside in a strong magnetic field (3–5 T), the atoms are very different from high-n Rydberg atoms with a Kepler orbit. More properly these weakly bound and strongly magnetized pairs are called guiding center drift atoms [4–6]. The characteristic cyclotron radius for the positron is much smaller than the separation between the positron and the antiproton. Likewise, the cyclotron frequency for the positron is much larger than the other dynamical frequencies for the atom. Under these circumstances, the rapid cyclotron motion may be averaged out, and the dynamics of the positron treated by guiding center drift theory. The dynamics is quasiclassical because the characteristic binding energy is much smaller than the Rydberg energy (typically 4 orders of magnitude smaller). References [5,6] provide an analysis of the internal dynamics of these novel atoms. Figure 1 shows the motion in the limit that is of interest here. The guiding center positron oscillates back and forth along the magnetic field in the Coulomb well of the antiproton and more slowly $\vec{E} \times \vec{B}$ drifts around the antiproton.

In this Letter, we discuss the motion of guiding center drift atoms in the electric and magnetic field of the plasma and trap. Starting with separate, but coupled, equations of motion for the positron and antiproton, we average over the rapid internal atom dynamics to obtain a single simplified equation of motion for the atom as a whole. This simplified equation represents a large reduction in the complexity of the dynamics.

We consider the simple case of a long positron plasma, where the space charge electric field is purely radial, $\vec{E} = \hat{\rho} E_\rho(\rho)$, and the magnetic field axial, $\vec{B} = \hat{z} B$. (This is a good approximation for the ATHENA geometry but not for the ATRAP geometry.) The simplified equation of motion then admits three constants of the motion (axial momentum, canonical angular momentum, and energy), and the atom dynamics is integrable.

The main result is that the weakly bound atoms are polarized by the electric field and can be trapped radially in the region of large electric field near the edge of the positron plasma. Recall that a polarizable material is attracted to a region of large electric field. To understand why the field is large near the plasma edge, recall that for a long positron column the radial space charge field increases linearly with radius ρ inside the plasma and then falls off like $1/\rho$ outside the plasma.

We will find a well depth of order $r^3 E_\rho^2/2$, where r is the characteristic radius of the atom, and E_ρ is the space charge field. Thus, the well is deeper and the trapping more effective for weakly bound atoms with relatively large r. The weakly bound atoms are more likely to emerge near the plasma ends, whereas the deeply bound atoms will emerge radially all along the column.

For simplicity, we start by considering the case where the amplitude of the field aligned oscillation is negligible compared to the cross field separation of the two particles. The cross field motion is then governed by the two

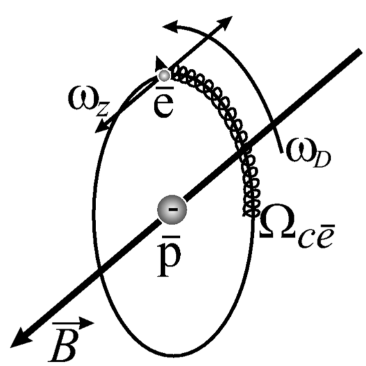

FIG. 1. Drawing of a guiding center atom. In order of descending frequency, the positron executes cyclotron motion, oscillates back and forth along a field line in the Coulomb well of the antiproton, and $\vec{E} \times \vec{B}$ drifts around the antiproton.

equations

$$m_{\bar{p}} \frac{d\vec{v}_{\bar{p}}}{dt} = -e\frac{\vec{v}_{\bar{p}} \times \vec{B}}{c} - \frac{e^2(\vec{r}_{\bar{p}} - \vec{r}_{\bar{e}})}{|\vec{r}_{\bar{p}} - \vec{r}_{\bar{e}}|^3} - e\vec{E}(\vec{r}_{\bar{p}}),$$
$$0 = e\frac{\vec{v}_{\bar{e}} \times \vec{B}}{c} - \frac{e^2(\vec{r}_{\bar{e}} - \vec{r}_{\bar{p}})}{|\vec{r}_{\bar{e}} - \vec{r}_{\bar{p}}|^3} + e\vec{E}(\vec{r}_{\bar{e}}), \quad (1)$$

where the positron inertia is neglected in the second equation as prescribed in the drift approximation.

It is convenient to introduce the transverse pseudomomentum [5,7]

$$\vec{P} = m_{\bar{p}}\vec{v}_{\bar{p}} - \frac{e}{c}\vec{r} \times \vec{B}, \quad (2)$$

where $\vec{r} = \vec{r}_{\bar{e}} - \vec{r}_{\bar{p}}$ is the relative position vector. The vector $\vec{r}$ is transverse to $\vec{B}$ since we neglect the field aligned motion of the positron relative to the antiproton. Adding the two equations of motion and Taylor expanding the electric field with respect to $\vec{r}$ yields the equation

$$\frac{d\vec{P}}{dt} = e(\vec{r} \cdot \vec{\nabla})\vec{E}. \quad (3)$$

We assume that the dimensions of the atom are small compared to the gradient scale for the field (i.e., $r/\rho_0 \ll 1$, where ρ_0 is the radius of a plasma column), and work only to first order in the gradient. In Eq. (3), $\vec{E} = \hat{\rho}E_\rho(\rho)$ is evaluated at an atom coordinate $\vec{\rho}$ that needs to be specified only to accuracy $\delta\rho \sim O(r)$.

To obtain a simplified equation of motion, we average Eq. (3) over the internal dynamics of the atom, obtaining the result

$$\frac{d\langle\vec{P}\rangle}{dt} = (\vec{d} \cdot \vec{\nabla})\vec{E}, \quad (4)$$

where $\vec{d} \equiv \langle e\vec{r}\rangle$ is the time-averaged dipole moment. Here, we assume that the period of the internal dynamics of the atom is short compared to the time for the atom as a whole to move a significant macroscopic distance. As we will see, this assumption is very well satisfied.

Since the right-hand side of Eq. (4) is already first order in the electric field gradient, we can evaluate $\vec{d}$ to zero order in the gradient. For a spatially uniform electric field, the energy (or Hamiltonian) for the pair is

$$H = \frac{m_{\bar{p}}v_{\bar{p}}^2}{2} - \frac{e^2}{r} - e\vec{r} \cdot \vec{E}. \quad (5)$$

Equation (3) implies that $\vec{P}$ is a constant of the motion for a uniform electric field, so we use Eq. (2) to eliminate $\vec{v}_{\bar{p}}$ in terms of $\vec{P}$, obtaining the result

$$H = \frac{P^2}{2m_{\bar{p}}} - \frac{e^2}{r} + \frac{e^2r^2}{2R^3} - e\vec{r} \cdot \left[\vec{E} + \frac{\vec{P} \times \vec{B}}{m_{\bar{p}}c}\right], \quad (6)$$

where $R^3 \equiv m_{\bar{p}}c^2/B^2$. Setting $\vec{P} = \langle\vec{P}\rangle$ in Eq. (6), and taking $\langle\vec{P}\rangle$ and H to be constant, yields an equation for the cross field orbit, that is, for $r = r(\theta)$, where (r, θ) are polar coordinates and $\theta = 0$ corresponds to the direction of the effective electric field $\vec{E}_{\rm eff} = \vec{E} + \langle\vec{P}\rangle \times \vec{B}/(m_{\bar{p}}c)$. When the effective field vanishes, which is the case for the motion shown in Fig. 1, the orbit is circular. When the field is nonzero, the orbit distorts in the direction of the field, and a nonzero time-average dipole moment exists. For a sufficiently small field, the distortion and dipole moment are linear in the field, and we can define the polarizability α, where $\vec{d} = \alpha\vec{E}_{\rm eff}$.

In the linear regime the orbit is given by $r = r_0 + \delta r(\theta)$, where

$$\delta r(\theta) = -\frac{r_0^3 E_{\rm eff}\cos\theta}{e[1 + (r_0/R)^3]}. \quad (7)$$

The time-average dipole moment is then given by

$$d = \frac{e\int_0^{2\pi}\frac{d\theta}{\dot{\theta}(r,\theta)} r\cos\theta}{\int_0^{2\pi}\frac{d\theta}{\dot{\theta}(r,\theta)}}, \quad (8)$$

where $\dot{\theta} = c/(eBr)\partial H/\partial r$ is the angular drift velocity associated with the relative motion, and r must be replaced by $r_0 + \delta r(\theta)$ everywhere in the integral. Linearizing in $E_{\rm eff}$ then yields the polarizability

$$\alpha = \frac{5}{2}r_0^3\frac{1 + \frac{2}{5}r_0^3/R^3}{(1 + r_0^3/R^3)^2}. \quad (9)$$

The expression for the angular velocity of the orbit drift motion, $\dot{\theta} = c/(eBr)\partial H/\partial r$, requires some explanation. Although expression (6) was written down as the energy of the two particles, it can be derived as a Hamiltonian for the relative motion [5]. From the Hamiltonian, one finds, not surprisingly, that the relative coordinate $\vec{r}$ undergoes drift motion in the effective potential H/e [i.e., $d\vec{r}/dt = c/(eB)\vec{\nabla}_r H \times \hat{z}$].

As discussed in Ref. [5], the nearly circular drift orbits considered here and shown in Fig. 1 are not the only possible motion for the pair. In a very weakly bound configuration, the positron $\vec{E} \times \vec{B}$ drifts in the field of the antiproton, and the antiproton $\vec{E} \times \vec{B}$ drifts in the field of the positron. These states, often referred to as giant dipole states [5,8,9], are not considered here. As mentioned in Ref. [5], an electric field gradient tends to separate (field ionize) such weakly bound pairs.

The time average of Eq. (3) and the definition $\vec{d} = \langle e\vec{r}\rangle$ yields the relation $\langle\vec{P}\rangle = m_{\bar{p}}\langle\vec{v}_{\bar{p}}\rangle - \vec{d} \times \vec{B}/c$. Substituting this expression into Eq. (4) and using the relation $\vec{d} = \alpha(\vec{E} + \langle\vec{P}\rangle \times \vec{B}/(m_{\bar{p}}c))$ yields the approximate equation of motion:

$$m_{\bar{p}}\frac{d\vec{v}}{dt} = \vec{\nabla}\frac{\alpha E^2}{2} + \alpha(\vec{\nabla}_\perp \cdot \vec{E})\frac{\vec{v} \times \vec{B}}{c}, \quad (10)$$

where $\vec{v} \simeq \langle\vec{v}_{\bar{p}}\rangle$ is the time-average velocity of the atom.

Taking the dot product of Eq. (10) with respect to $\vec{v}$ and integrating over time yields an equation for conservation of energy:

$$\frac{m_{\bar{p}}v^2}{2} - \alpha\frac{E^2}{2} = \text{const.} \quad (11)$$

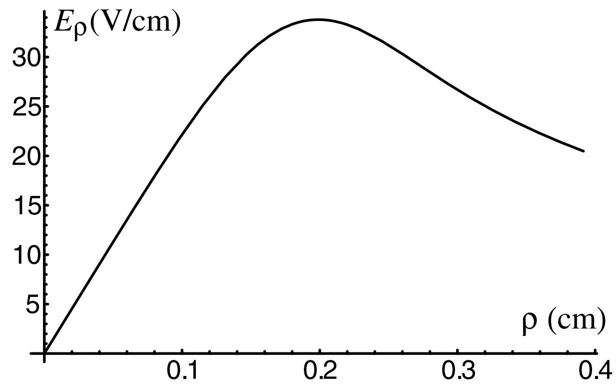

FIG. 2. Radial profile of the space charge electric field.

As one would expect, all of the Lorentz force terms drop out of the equation for conservation of energy. For the case where the electric field is radial, $\vec{E} = \hat{\rho}E_\rho(\rho)$, Eq. (10) yields an equation for conservation of canonical angular momentum

$$\text{const} = L = \left(m_{\bar{p}} v_\varphi \rho + \frac{B}{c}\rho\alpha E_\rho\right)\left(1 - \frac{\alpha B^2}{m_{\bar{p}}c^2}\right)^{-1}. \quad (12)$$

Here, (ρ, φ) are polar coordinates for the plasma column. Using Eq. (12) to eliminate v_φ in favor of the constant $L' \equiv L[1 - \alpha B^2/(m_{\bar{p}}c^2)]$ in Eq. (11) yields the result

$$\frac{m_{\bar{p}}}{2}v_\rho^2 + \frac{1}{2m_{\bar{p}}\rho^2}\left(L' - \frac{B}{c}\rho\alpha E_\rho\right)^2 - \alpha\frac{E_\rho^2}{2} = \text{const}. \quad (13)$$

Next, we use the approximate equation of motion to follow the orbit of a guiding center atom moving in the positron plasma. We choose a plasma density $n_0 = 2.5 \times 10^8\ \text{cm}^{-3}$ and plasma radius $\rho_0 = 0.2$ cm in accord with ATHENA parameters, and for convenience take the (unknown) density profile to be simply $n(\rho) = n_0 \exp[-(\rho/\rho_0)^4]$. For a long column, the corresponding space charge field is shown in Fig. 2. Also, in accord with ATHENA parameters we choose the magnetic field strength $B = 3$ T.

Figure 3 shows the orbit of a rather tightly bound guiding center atom ($r = 2.4 \times 10^{-5}$ cm, $e^2/r = 5.9$ meV) ejected in the azimuthal direction with rather small initial velocity $v_\varphi = 2.4 \times 10^3$ cm/s. The figure actually shows two nearly identical curves. The solid curve is the solution to approximate Eq. (10) using the polarizability $\alpha = 3.6 \times 10^{-14}\ \text{cm}^3$, and the dashed curve is the ion orbit in the solution to coupled (exact) Eqs. (1). This latter solution is difficult computationally since about a million cycles of the internal dynamics must be followed. The rapid internal dynamics has been averaged out in approximate Eq. (10). For this case of relatively tight binding and, consequently, shallow radial well, only atoms with small initial velocity are trapped. For example, had the atom been given initial velocity 1.6×10^4 cm/s, it would have escaped.

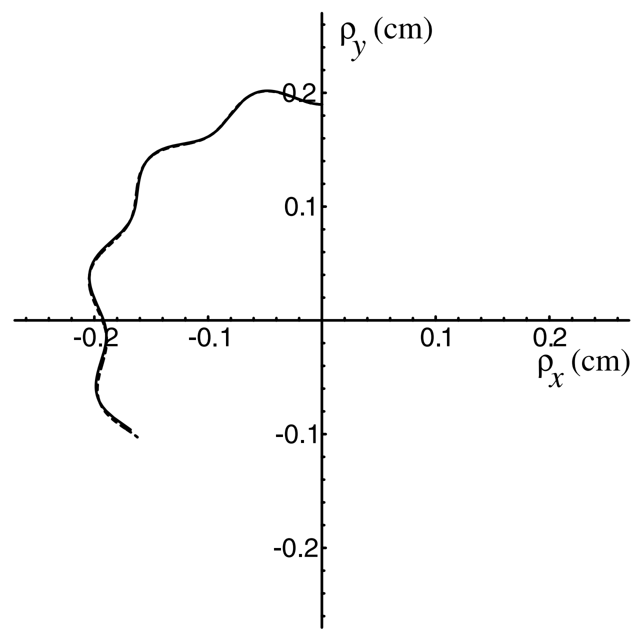

FIG. 3. Trapping of a rather tightly bound atom ejected with small azimuthal velocity. The dashed curve is the solution of the coupled Eqs. (1), and the solid curve is the solution of the approximate Eq. (10) using the polarizability $\alpha = 3.6 \times 10^{-14}\ \text{cm}^3$.

More shallowly bound atoms experience a deeper well and are confined for larger initial velocity. However, the more shallowly bound atoms are closer to field ionization, and the dipole moment becomes a nonlinear function of the electric field. Figure 4 shows a plot of $\alpha(E_\rho)/\alpha_L$ versus E_ρ, where the linear value, α_L, is given by Eq. (9) for the case of a circular orbit of radius $r_0 = 4.0 \times 10^{-5}$ cm. For small E_ρ (less than 15 V/cm), α is constant, indicating a linear relation between the polarization and field. However, for large E_ρ, $\alpha(E_\rho)$ increases with E_ρ as field ionization is approached.

Figure 5 shows the orbit of a more loosely bound drift atom ($r = 4.0 \times 10^{-5}$ cm, $e^2/r = 3.6$ meV) with a larger

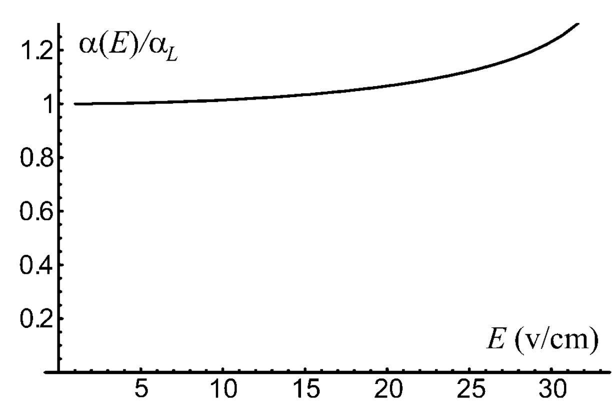

FIG. 4. Scaled polarizability versus electric field. Here α_L is given in Eq. (9) for $r = 4.0 \times 10^{-5}$ cm.

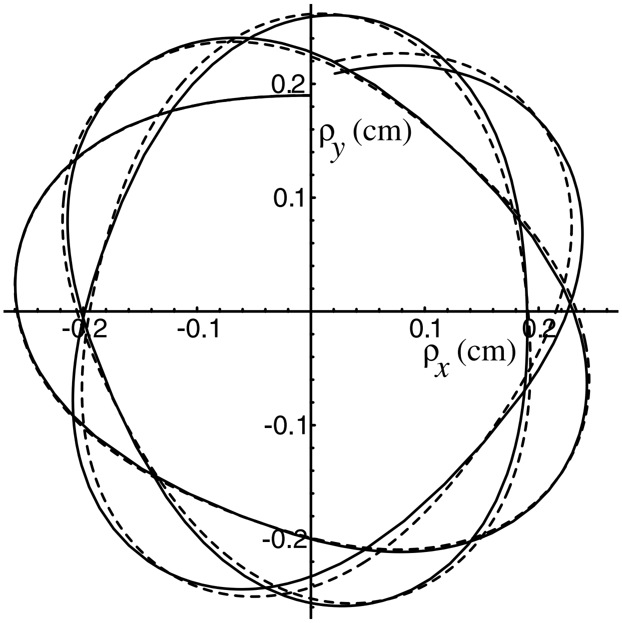

FIG. 5. Trapping of guiding center atom with higher initial velocity and shallower binding than in Fig. 3. The dashed curve is the solution of coupled Eqs. (1). The continuous curve is the solution of approximate Eqs. (10) with $\alpha = 1.18\alpha_L$.

initial velocity ($v_\varphi = 2.7 \times 10^4$ cm/s). This velocity corresponds to initial antiproton kinetic energy $m_{\bar{p}} v_\varphi^2/2 =$ 0.38 meV, as compared to a 1.3 meV temperature quoted for some ATHENA experiments. In this case, the polarization is in the nonlinear regime, and approximate Eq. (10) was solved for the polarizability $\alpha = \alpha(E \simeq 25\ \mathrm{V/cm}) = 1.18\alpha_L = 1.8 \times 10^{-13}\ \mathrm{cm}^3$. Again the solid curve is the solution to Eq. (10), and the dashed curve the solution to coupled Eqs. (1). In this case, the two curves are close, but can be distinguished, presumably because the nonlinear polarizability function $\alpha(E)$ was approximated by a single value, $\alpha(25\ \mathrm{V/cm}) \simeq 1.18\alpha_L$. Both curves show that the atom is confined radially.

Thus far, we considered the simple case where the amplitude of the field aligned oscillations, z, is negligibly small compared to r. For finite, but small z/r, Eq. (9) for α is replaced by

$$\alpha = \frac{5}{2} r^3 \frac{1 + \frac{2}{5}\frac{r^3}{R^3} - \frac{33}{40}\frac{z^2}{r^2}}{(1 + \frac{r^3}{R^3} - \frac{3}{4}\frac{z^2}{r^2})^2}. \quad (14)$$

The polarizability increases with z because a guiding center atom is less tightly bound when the amplitude of the axial bounce motion increases. However, for fixed binding energy α decreases as z increases, to keep the binding energy fixed, and the net result is a decrease in α.

For sufficiently deep binding (i.e., $r^3 = R^3 m_{\bar{e}}/m_{\bar{p}}$), the drift approximation for the positron motion breaks down [5]. The cyclotron frequency, frequency of field aligned oscillations, and the $\vec{E} \times \vec{B}$ drift rotation frequency all become comparable, and the internal dynamics of the atom becomes chaotic [5,10]. Although our calculation of α fails, one still expects the chaotic atom to be characterized by a polarization of order $\alpha \sim r^3$, where r is the characteristic radius of the atom, and the basic trapping mechanism to be applicable.

Finally, we note that replacing the space charge field of the other positrons by the mean field, $\vec{E} = E(\rho)\hat{\rho}$, omits important physics. The weakly bound atom occasionally has a close collision with a positron, and the collision can produce reionization or deeper binding. This is the subject of three-body recombination and the collisional cascade to deeper binding [4]. The analysis here follows the motion of the weakly bound atom between the relatively rare close collisions.

This work was supported by National Science Foundation Grant No. PHY9876999 and Office of Naval Research Grant No. N00014-96-1-0239. The authors wish to thank Dr. Lars Jørgensen and Professors Gerald Gabrielse and Fred Driscoll for helpful discussions.

[1] M. Amoretti *et al.*, Nature (London) **419**, 456 (2002).
[2] G. Gabrielse *et al.*, Phys. Rev. Lett. **89**, 213401 (2002).
[3] G. Gabrielse *et al.*, Phys. Rev. Lett. **89**, 233401 (2002).
[4] M. E. Glinsky and T. M. O'Neil, Phys. Fluids B **3**, 1279 (1991).
[5] S. G. Kuzmin, T. M. O'Neil, and M. E. Glinsky, Phys. Plasmas **11**, 2382 (2004).
[6] D. Vrinceanu, B. E. Granger, R. Parrott, H. R. Sadeghpour, L. Cederbaum, A. Mody, J. Tan, and G. Gabrielse, Phys. Rev. Lett. **92**, 133402 (2004).
[7] J. E. Avron, I. W. Herbst, and B. Simon, Ann. Phys. (N.Y.) **114**, 431 (1978).
[8] O. Dippel, P. Schmelcher, and L. S. Cederbaum, Phys. Rev. A **49**, 4415 (1994).
[9] J. Shertzer, J. Ackermann, and P. Schmelcher, Phys. Rev. A **58**, 1129 (1998).
[10] J. B. Delos, S. K. Knudson, and D. W. Noid, Phys. Rev. A **30**, 1208 (1984).